

# Intrusion Simulation of a C60 Ball into Sliding Contact Space with Graphene Layered Surfaces

Zhang Qi, Diao Dongfeng, Li Pei

Key Laboratory of Education Ministry for Modern Design and Rotor-Bearing System, School of Mechanical Engineering, Xi'an Jiaotong University, Xi'an 710049, China

**Abstract:** The intrusion process of a C60 molecular ball into a sliding contact space with graphene layered surfaces was simulated using the Molecular Dynamic approach. The contact space was made up by two silicon substrates with graphene layered on the surface of the upper substrate forming an included angle which was defined as initial entry angle changing from 20° to 90°. Then a linear velocity of 30Å/ps was applied to the lower substrate along horizontal direction. The simulation was carried out using Tersoff potential of C and Si atoms at room temperature 300K. The simulation results showed that when the intrusion angle exceeded a critical angle of 80°, the C60 ball could not intrude the contact space, and the number of the sticking atoms sharply increased. Also, the dependence of maximum pull-off force acting on the upper substrate on the initial entry angle during the C60 intrusion process was calculated in which the critical force for C60 intrusion is found. All the results showed that the upper silicon substrate was well protected by the mono graphene layer.

**Key words:** Molecular dynamic simulation; Sliding contact space; C60; Graphene layer; Critical angle; Critical force

Graphene has attracted a lot of attentions because of its excellent electrical and mechanical properties since it is first experimentally prepared in 2004<sup>[1-2]</sup>. Its intrinsic strength is predicted to exceed that of any other material, and it may be the promising material for controlling the wear and the fracture caused by surface stresses<sup>[3-5]</sup>. This enables graphene to be nanomechanical material, especially to be the protective layer to nanoelectromechanical system (NEMs). In this work, graphene layer is used to forming a sliding contact space in which C60 intruding it to research the influence of graphene layer on a particle intruding process.

The interactions between particles and substrates have been investigated extensively using both experiments and atomistic simulation methods. Many studies focus on the experimental investigations about the phenomena of particles interacting with substrates in micro scale with the help of AFM<sup>[6-8]</sup>. T R Ramachandran et al. successfully controlled the 3-D features via nanomanipulation of Au particles in 5–27 nm diameters on a surface using NC-AFM and showed that repulsive forces could move these particles<sup>[6]</sup>. M. D. M. Peri et al. got the experimental evidence for the existence of the rolling resistance moment, and measured the adhesion between a spherical particle and a flat surface<sup>[7-8]</sup>.

As mentioned above, it is found that without AFM, the experiments about researching the motion of particle in the

nanometer scale system will be difficult to observe. So molecular dynamics simulation as a powerful computational method is widely used to understand the interface behaviors between particles and substrates in atom scale<sup>[9-12]</sup>. P. Li and D. F. Diao observed the intrusion process of C60 ball into the Si sliding contact space, and a critical initial entry angle is calculated<sup>[10]</sup>. N. Sasaki et al. have developed “C60 molecular bearing” in which the close-packed C60 particles were inserted between two parallel rigid graphite sheets, and clarified that three-dimensional degree of C60 motion leads to ultra low friction by MD simulation<sup>[11-12]</sup>. The interaction of energetic fullerene molecules with silicon crystal surface has been studied<sup>[13-14]</sup>, and Tersoff Si/C potential was used to model the interaction between the C and Si atoms<sup>[13]</sup>.

In this study, Molecular Dynamic approach is used to simulate the intrusion process of C60 into the sliding contact space in which a velocity of 30Å/ps (3.0 km/s, which can be accepted in space station where the orbital speed is 7.5km/s<sup>[15]</sup>) is applied to the tribosystem. The intrusion process is observed, after that the numbers of sticking atoms as well as the pull-off forces of the upper substrate are calculated.

## 1 Experiment

### 1.1 Computational model

We carried detailed molecular dynamics simulations to de-

scribe the nano-scaled intrusion process of C60 into the sliding contact space formed by two substrates layered by a graphene on the surface of the upper substrate.

Fig. 1 shows the model of C60 ball-substrates intrusion system. The lower substrate is positioned horizontal, while the upper substrate is inclined forming an initial entry angle  $\alpha$  ranging from 20° to 90°. C60 is intercalated in the contact space. The initial position of the C60 ball was located in the space at the position where the ball contacted with the lower substrate, but not contact with the upper substrate, i.e. the minimum distance between the atom in C60 and in lower substrate equaled to the cutoff distance 2.4Å which was calculated by  $R_{ij}=(R_iR_j)^{1/2}$  (here  $R_i=1.8\text{\AA}$  for C,  $R_j=2.7\text{\AA}$  for Si ); the minimum distance between the atom in C60 and in upper substrate equaled to the cutoff distance 1.8Å.

Here we employed the lower substrate with dimensions  $A_1 \times B_1 \times C_1=108.6\text{\AA} \times 43.4\text{\AA} \times 16.29\text{\AA}$  containing 4359 atoms of silicon (100) with the lattice constant equals 5.43Å, while the upper Si substrate with dimensions  $A_2 \times B_2 \times C_2=48.87\text{\AA} \times 21.72\text{\AA} \times 10.86\text{\AA}$  containing 715 atoms. And the size of the graphene layer is  $A_3 \times B_3 \times C_3=47.97\text{\AA} \times 21.30\text{\AA} \times 1.4\text{\AA}$  (the diameter of the C is 1.4Å) with 420 carbon atoms.

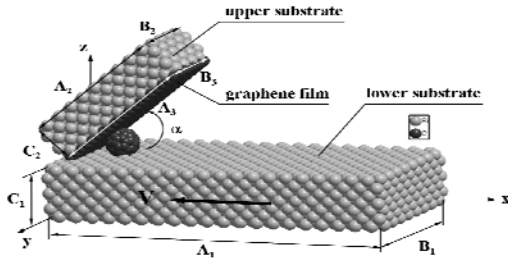


Fig. 1 Schematic sketch of MD model: C60 ball-substrates intrusion system with graphene film

## 1.2 Calculated methodology

In these simulations, the Tersoff potential function is also employed to the interaction among Si atoms and C atoms. The total Tersoff energy  $E$  can be expressed as in the Equation (1).

$$E = \sum_i E_i = \frac{1}{2} \sum_{i \neq j} V_{ij} \quad (1)$$

As  $j$  and  $k$  are assumed to be the neighboring atoms of atom  $i$ , then  $V_{ij}$  is the bond energy, so the summation in the equation is over all the atomic bonds in the control volume.  $V_{ij}$  is a function of the repulsive pair potential  $f_R$  and the attractive pair potential  $f_A$ , and has the form

$$V_{ij} = f_c(r_{ij}) [f_R(r_{ij}) + b_{ij} f_A(r_{ij})] \quad (2)$$

Where the atomic bond lengths of atoms  $i-j$  and  $i-k$  are  $r_{ij}$  and  $r_{ik}$ , and

$$f_R(r_{ij}) = A_{ij} \exp(-\lambda_{ij} r_{ij}), \quad f_A(r_{ij}) = -B_{ij} \exp(-\mu_{ij} r_{ij});$$

$$f_c(r_{ij}) = \begin{cases} 1, & r_{ij} < R_{ij}, \\ 0.5 + 0.5 \cos \pi [(r_{ij} - R_{ij}) / (S_{ij} - R_{ij})], & R_{ij} < r_{ij} < S_{ij}, \\ 0, & r_{ij} > S_{ij}; \end{cases}$$

$$b_{ij} = \chi_{ij} (1 + \beta_i^n \zeta_{ij}^n)^{-1/2n},$$

$$\zeta_{ij} = \sum_{k \neq i, j} f_c(r_{ik}) g(\theta_{ijk});$$

$$g(\theta_{ijk}) = 1 + c_i^2 / d_i^2 - c_i^2 / [d_i^2 + (h_i - \cos \theta_{ijk})^2];$$

$$\lambda_{ij} = (\lambda_i + \lambda_j) / 2, \quad \mu_{ij} = (\mu_i + \mu_j) / 2, \quad A_{ij} = (A_i A_j)^{1/2};$$

$$B_{ij} = (B_i B_j)^{1/2}, \quad R_{ij} = (R_i R_j)^{1/2}, \quad S_{ij} = (S_i S_j)^{1/2}.$$

Other parameters such as  $A$ ,  $B$ ,  $R$ ,  $S$ ,  $\lambda$ ,  $\chi$  and  $\mu$ , as listed in Table 1, with equations (1) and (2), the interaction forces between silicon atoms and carbon atoms can be obtained by calculating the gradient of total Tersoff energy  $E^{[16-17]}$ .

The NVE ensemble is evolved to the molecular dynamics simulations, and the simulations were conducted using free boundary conditions. And the outmost one layer of atoms around the lower substrate are rigid atoms; meanwhile the atoms on the rightmost one layer of the upper silicon base and graphene are fixed; while the rest of the atoms in the simulation system was treated unfixed as thermostat atoms at 300 K by rescaling their velocities. The lower substrate was then subjected to a constant velocity of 30Å/ps in the negative X-direction, and the lower substrate was moved for 3000 steps at a time step of 0.001ps, this means that the effective displacement of the lower substrate per step was 0.03Å.

Table 1 Parameters in Tersoff potential for carbon and silicon<sup>[16]</sup>

Material	C	Si
A (eV)	1.3936×10 <sup>3</sup>	1.8308×10 <sup>3</sup>
B (eV)	3.467×10 <sup>2</sup>	4.7118×10 <sup>2</sup>
$\lambda$ (Å <sup>-1</sup> )	3.4879	2.4799
$\mu$ (Å <sup>-1</sup> )	2.2119	1.7322
$\beta$	1.5724×10 <sup>-7</sup>	1.1000×10 <sup>-6</sup>
n	7.2751×10 <sup>-1</sup>	7.8734×10 <sup>-1</sup>
c	3.8049×10 <sup>4</sup>	1.0039×10 <sup>5</sup>
d	4.384×10 <sup>0</sup>	1.6217×10 <sup>1</sup>
h	-5.7058×10 <sup>-1</sup>	-5.9825×10 <sup>-1</sup>
R(Å)	1.8	2.7
S(Å)	2.1	3.0
$A_f / ^\circ\text{C}$	$\chi_{\text{Si-Si}}=1.0$	$\chi_{\text{C-Si}}=0.9776$

## 2 Results and Discussion

### 2.1 Intrusion process

The initial entry angle  $\alpha$  is found to be an important factor to the intrusion process of C60. So we repeated the simulation every 2° from 20° to 90°.

The intrusion processes of C60 at different time steps from 200 to 2600 with the initial entry angle equals to 40°, 80° and 82° are shown in Fig. 2, Fig. 3 and Fig. 4, respectively.

In Fig. 2, for  $\alpha=40^\circ$ , C60 first sticks to the lower substrate surface and then moved together with it along the negative

X-direction when the constant velocity is applied to the lower substrate. Then the upper substrate starts to bend and is lift by the compression force of C60 (Fig. 2b-Fig. 2f), then C60 passes the sliding contact space (Fig. 2g). From Fig. 2g, we can see that the entry angle is slightly becoming smaller. Because of the interaction between C60 and the lower substrate, some atoms on the lower substrate surface are forced to leave their original positions, and stick to C60. The fallen atoms will adhere to the upper substrate if they move toward the upper substrate to a distance less than 2.7Å or 2.4Å (cutoff distance between C-C and C-Si). However, due to the protection of the graphene layer, the upper substrate has no atom loss.

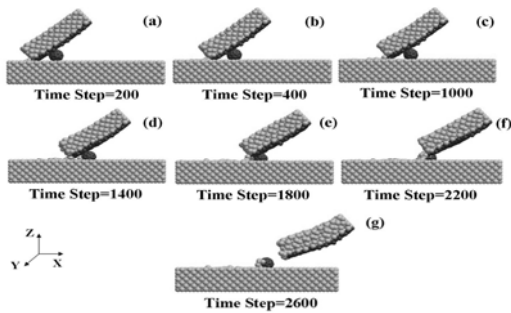


Fig. 2 MD simulation results for  $\alpha=40^\circ$

As is defined: atoms which have moved a distance more than the cutoff distance (the cutoff distance of C-C and Si-Si are 1.8Å and 2.7Å respectively) from their initial positions are called sticking atoms. When the initial intrusion angle is 40°, 12 sticking atoms of the lower substrate are calculated, but there is no sticking atom of the upper substrate. During the whole intrusion process, C60 and the graphene layer keep intact, and both sliding and rolling movements of C60 are observed.

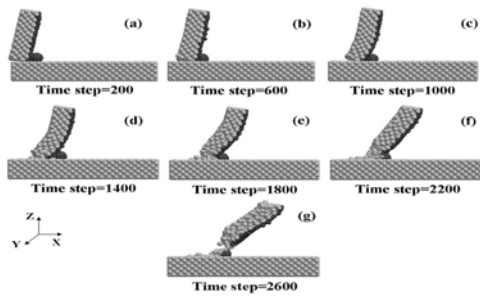


Fig. 3 MD simulation results for  $\alpha=80^\circ$

Compared to the simulation results of C60 intrusion process at the initial entry angle of 40°, there are some different phenomena of the process when the initial entry angle is 80°. As shown in Fig. 3, when the C60 is coming closer to the upper substrate, the upper substrate is lift and bends obviously, and then the entry angle is becoming about 60° which is much smaller than 80° (Fig. 3g). In Fig. 3f, we can clearly see that a

lot of atoms near the contact area leave the upper and lower substrates. Fig. 3g demonstrates that with the increasing intrusion time steps, C60 can intrude the sliding contact space leading to much larger number of sticking atoms of both upper and lower substrate. This means the damage of both upper and lower substrate is more serious. After the simulation, there are 9 sticking atoms of the lower substrate, and 16 sticking atoms of the upper substrate.

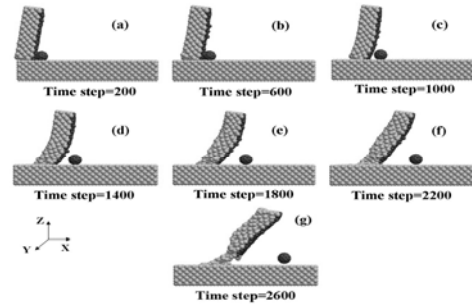


Fig. 4 MD simulation results for  $\alpha=82^\circ$ .

Fig. 4 shows the C60 intrusion process at the initial entry angle of 82°. In this case, more sticking atoms from the upper and lower substrate are adhering together (Fig. 4g), so the upper substrate is pulled by the moving lower substrate and stop C60 intruding the sliding space. There is more atom loss of the upper and lower substrates (the number of sticking atoms is 14 and 16 respectively). On the other hand, it is observed that when the initial intrusion angle  $\alpha > 80^\circ$ , C60 can not intrude the sliding contact space.

## 2.2 Critical intrusion angle and force

Fig. 5 shows the number of sticking atoms (which moved a distance more than the cutoff distance 2.7Å from their initial positions) of the lower substrate (fig. 5a) and the upper substrate (fig. 5b) at different initial entry angles. The number of the sticking atoms of the lower substrate changes irregularly with the increasing initial entry angle (Fig. 5a). There are up to 22 sticking atoms when the initial entry angle is 52°, and the average number is 11. The data points in Fig. 5b can be divided into two regions. When the initial entry angle is less than 80°, the number of sticking atoms of the upper substrate is less than 10, even in most cases there is no sticking atom. When the initial entry angle is over 80°, the number of sticking atoms of the lower substrate increased sharply as the max force of the upper substrate suddenly becomes much larger. So, in this study,  $\alpha=80^\circ$  is the critical intrusion entry angle, which means when the initial entry angle is larger than 80°, the C60 can not intrude into the sliding contact space and there will be much more sticking atoms of the upper substrate.

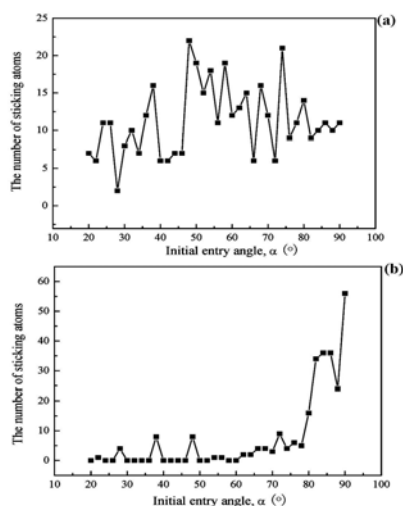


Fig. 5 (a) Number of sticking atoms of the upper substrate with the increasing initial; (b) Number of sticking atoms of the lower substrate with the increasing initial entry angle

Fig. 6 shows the max pull-off forces of the upper substrate changes with the increasing initial entry angles. It is demonstrated that when the initial entry angle is less than  $80^\circ$ , the mean max pull-off force is about 80nN, but when the initial entry angle is over  $80^\circ$ , the max pull-off force sharply increases to 110nN. From Fig. 5b and Fig. 6, we can see with the increasing initial entry angle the force of the upper substrate has substantially similar change trend to that of the number of sticking atoms, and the critical intrusion force is found to be 110nN, which means when the max pull-off is more than 110nN, the number of sticking atoms of the upper substrate rapidly increases, and C60 can not intrude into the contact space.

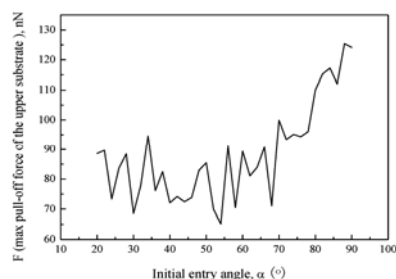


Fig. 6 The max force of the upper substrate changes with the increasing initial entry angle

In our previous study<sup>[10]</sup>, the upper substrate was purely made up of silicon atoms without the graphene layer, the number of sticking atoms of the upper substrate was up to 50 when the entry angle was  $70^\circ$ , with the increasing of the initial entry angle the number of sticking atoms reached to as many as 550. On the contrary, when the surface of upper substrate is layered by graphene, there are at most 56 sticking atoms, because the strength of the upper substrate is remarkably im-

proved. This is very important at the industrial point view.

### 3 Conclusions

Molecular Dynamic simulation is used to study the intruding process of a C60 molecular ball into a sliding contact space with graphene layered surfaces.

1) The critical initial entry angle is found to be  $80^\circ$ . With increasing initial entry angle, the number of sticking atoms of the upper substrate is divided into two regions.

2) The critical intrusion pull-off force is found to be 110nN. When the intrusion pull-off force is less than the critical value, C60 can intrude into the sliding contact space and a small number of sticking atoms are produced. Inversely, the number of sticking atoms of the upper substrate is suddenly increased and C60 can not intrude.

Compared to our previous work, the number of sticking atoms of the upper substrate is decreased obviously, which demonstrates that the graphene layer can well protect the upper substrate.

### References

- Novoselov K S, Geim A K, Morozov S V et al. *Science*[J], 2004, 306(5696): 666
- Geim A K, Novoselov K S. *Nature Materials*[J], 2007(6):183
- Diao D F, Sawaki Y. *Thin Solid Films*[J], 1995, 270: 362
- Diao D F, Sawaki Y, Suzuki H. *Surface & Coating Technology*[J], 1996, 86-87: 480
- Diao D F, Kato K. *Thin Solid Films*[J], 1994, 245: 104
- Ramachandran T R, Baur C, Bugacov A et al. *Nanotechnology*[J], 1998, 9(3): 237
- Peri M D M, Cetinkaya C. *Philosophical Magazine*[J], 2005, 85(13): 1347
- Ding W, Howard A J, Peri M D M et al. *Philosophical Magazine*[J], 2007, 87(36): 5685
- Valentini P, Dumitrica T. *Journal of Nano Research*[J], 2008, 1: 31
- Li P, Diao D F. *Lubrication Science*[J], 2011, accepted for publication, DOI: 10.1002/lis.163
- Miura K, Kamiya S, Sasaki N. *Physical Review Letters*[J], 2003, 90(5): 055509
- Sasaki N, Itamura N, Miura K. *Japanese Journal of Applied Physics*[J], 2007, 46(49): L1237
- Beardmore K, Smith R, Webb R P. *Modelling and Simulation in Materials Science and Engineering* [J], 1994, 2(3): 313
- Smith R, Beardmore K, Gras-Marti A. *Vacuum*[J], 1995, 46(8): 1195
- Krick B A, Sawyer W G. *Tribology Letters*[J], 2011, 41(1): 303
- Tersoff J. *Physical Review B*[J], 1988, 37(12): 6991
- Tersoff, J. *Physical Review B*[J], 1989; 39(8): 5566